Available online at www.sciencedirect.com

ScienceDirect

Scripta Materialia 72–73 (2014) 55–58

Scripta MATERIALIA

www.elsevier.com/locate/scriptamat

# Measurement of uncertainty in orientation distribution function calculations

A. Creuziger,[a,*] K. Syed[b] and T. Gnäupel-Herold[a]

[a]National Institute of Standards and Technology, 100 Bureau Dr., Gaithersburg, MD 20899, USA
[b]University of Maryland, College Park, MD 20742, USA

Received 17 September 2013; accepted 18 October 2013
Available online 26 October 2013

A technique to quantify the uncertainty in an estimated orientation distribution function (ODF) by propagating the uncertainty from measured pole figures is demonstrated in this paper using Monte Carlo techniques and the Matlab toolbox for quantitative texture analysis. Unlike the uncertainty in the measured pole figures, where small values of intensity correlate to high uncertainty, uncertainty as a function of orientation in an ODF is not directly related to intensity.
Published by Elsevier Ltd. on behalf of Acta Materialia Inc.

*Keywords:* Neutron diffraction; Texture; Monte Carlo simulation; Ferritic steels

The field of texture analysis has been described as "quantitative" for over 30 years [1–4]. Techniques to measure crystallographic texture have been widely used to measure preferred crystallographic orientations. The crystallographic information is often described in pole figures or orientation distribution functions (ODFs). Pole figures display the concentration of orientations of a fixed (*h k l*) crystal axis as a function of spatial orientation. Pole figure descriptions are incomplete in that the rotation about the fixed axis is not shown. ODFs present a way to show the complete orientation data.

Two major classifications of techniques to estimate ODFs exist: direct and indirect. Direct methods for estimating an ODF use a series of measurements of the complete orientation information spatially (such as electron backscatter diffraction). Indirect methods typically rely on comparisons between pole figures provided as an input to a solver and pole figures generated from an estimated ODF. Some examples of indirect methods are harmonic[1] [5], WIMV [6], ADC [7] and the Matlab toolbox for quantitative texture analysis (MTEX) [8].

Estimates of the precision and accuracy in crystallographic texture measurements such as pole figures and ODFs have not been widely used. Uncertainty in pole figure measurements have been previously investigated by Nikolayev et al. [9] and Lychagina et al. [10]. These are based on time-of-flight (TOF) neutron-diffraction measurements to estimate the effect of counting time on the pole-figure quality. The article by Mücklich and Klimanek [11] summarizes some of the sources of uncertainty in quantitative texture analysis, particularly for X-ray-based diffraction measurements.

Prior attempts to assess uncertainty in ODF measurements have focused on errors in the solver techniques. For indirect ODF estimation methods, the effect of a finite number of pole figures [4], truncation [4,8] and "ghost correction" [12] are widely known sources of uncertainty. Similarly, bias errors and disagreement between solvers are widely known issues [1]. One approach to assessing the difference between models is to check the solver using standard orientation distribution functions [13,14] or known texture functions [15]. For direct solvers, other problems, such as the effect of grain statistics, the non-equiaxed nature of grain shape and spatial correlations between grains, have been considered theoretically [16], but more experimental work is needed.

As described, a variety of sources of uncertainty exist in estimated ODFs: random errors from the pole figure measurements, truncation errors from the finite number of pole figures or the finite range of accessible reflections (X-ray), and differences between ODF solver techniques.

* Corresponding author. Tel.: +1 3019756015; e-mail: adam.creuziger@nist.gov

[1] Certain commercial equipment, instruments or materials are identified in this paper in order to specify the experimental procedure adequately. Such identification is not intended to imply recommendation or endorsement by the National Institute of Standards and Technology, nor is it intended to imply that the materials or equipment identified are necessarily the best available for the purpose.

1359-6462/$ - see front matter Published by Elsevier Ltd. on behalf of Acta Materialia Inc.
http://dx.doi.org/10.1016/j.scriptamat.2013.10.017

The focus of this work is assessing the first source; specifically, how random errors in the intensity data of pole figures from counting statistics propagate into the orientation distribution function.

Estimates of the uncertainty of an ODF are crucial for many reasons. ODFs are commonly used as a qualitative comparison metric. An assessment of uncertainty is a necessary component to determine if the difference between two (or more) estimated ODFs is significant. Uncertainty for extracted values such as volume fractions are also important as the volume fraction of a given orientation is often used when comparing two ODFs.

Monte Carlo techniques are used to propagate the uncertainty in computational models, and rely on taking pseudo-random draws from a probability distribution [17,18]. When employed in error analysis or uncertainty analysis, the input variables are perturbed in a manner consistent with their uncertainty and the perturbed input variables are used to create a new output value. The input variables are repeatedly perturbed in this manner to create an ensemble of output values. The ensemble of output values can then be used to summarize the variation in the output. Morawiec has explored this approach for ODFs where model pole figures are perturbed in a similar manner [15]. However, in Ref. [15] only the uncertainty in the overall texture function was considered; the effect on individual orientations in the ODF was not.

Complete pole figures for an undeformed SAE 1008 steel sample were collected using the BT-8 residual stress diffractometer at NIST [19]. Neutron diffraction was chosen so that complete pole figures could be measured, nullifying the effect of incomplete pole figures as a source of uncertainty. SAE 1008 steel is a ferritic steel with a body-centered cubic crystal structure. The (200), (110) and (211) reflection planes (**h**) were measured using a hexagonal mesh approximately equivalent to a 5° angular spacing [20]. Each point in the pole figure ($\alpha$,$\beta$) is determined by stereographic projection of the reflection vector (**r**) onto a two-dimensional surface. The number of diffracted neutrons (counts) at each point $(\alpha, \beta)$ on the pole figure is referred to as the peak counts $N_p$, determined by subtracting the integrated intensity of the background $N_b$ from that of the total number of counts $N_t$:

$$N_p = N_t - N_b \tag{1}$$

The pole figure data, $P(\mathbf{h},\mathbf{r})$, is therefore a plot of the number of peak counts as a function of the reflection plane and the orientation of the sample, calculated from the total and background counts:

$$P(\mathbf{h},\mathbf{r}) = P_t(\mathbf{h},\mathbf{r}) - P_b(\mathbf{h},\mathbf{r}) \tag{2}$$

The numbers of total and background counts are both expected to follow a Poisson distribution. The relative standard deviation of the number of peak counts is then:

$$\sigma_p = \frac{\sqrt{N_t} + \sqrt{N_b}}{N_t - N_b} \tag{3}$$

The program PeakFit (PF) [21] was used to analyze the experimental pole figure data. At each point on the pole figure, the diffraction peak was fitted with a Gaussian peak and a constant background. The total number of counts and the background number of counts at each point in the pole figure measurement were calculated and exported to the crystallographic texture analysis package MTEX.

MTEX was used to estimate the ODFs. Using the nomenclature of MTEX, a set of Euler angles was defined as an "orientation" (**g**). The orientation was then used to determine the "center" of a kernel function. For the analysis presented here, the de la Vallee–Poussin kernel and 5° half width were used. The choice of half width resulted in 1232 radially symmetric kernel functions distributed to fill Euler space.

MTEX uses a finite mixture of a uniform texture distribution ($\mathbf{g}_u$) and radially symmetric kernel functions ($\mathbf{g}_i$) to approximate the ODF $f(\mathbf{g})$. The radially symmetric kernel functions are centered on a grid in the ODF space (Bunge Euler angles: $\varphi_1$, $\Phi$, $\varphi_2$) in defined locations determined by the half-width of the kernel function. In order to indicate the relative proportion of each of the radially symmetric kernel functions, each radially symmetric kernel function has a corresponding "weight" value ($a_i$). The ODF is then represented as a series of the uniform and radially symmetric kernel functions:

$$f(\mathbf{g}) = a_u\mathbf{g}_u + \sum_1^i a_1\mathbf{g}_1 + a_2\mathbf{g}_2 \ldots + a_i\mathbf{g}_i \tag{4}$$

The term "intensity" for an ODF is the ratio of weight at a given orientation relative to the weight of the same orientation in a uniform (or random) texture distribution, with units of multiples of uniform distribution (MUD), like the pole figures. The details of the calculation from pole figure to ODF are described by Hielscher and Schaeben [8].

A Monte Carlo technique was used to estimate the uncertainty in the estimated ODF due to the uncertainty in the pole figure measurements. This technique was applied by perturbing each point in the pole figure $P(\mathbf{h},\mathbf{r})$. A Poisson pseudo-random number generator (poissrnd) was applied to the total and background counts at each point and then subtracted to generate the perturbed pole figure data $\hat{P}_N(\mathbf{h},\mathbf{r})$:

$$\hat{P}_N(\mathbf{h},\mathbf{r}) = \text{poissrnd}(P_t(\mathbf{h},\mathbf{r})) - \text{poissrnd}(P_b(\mathbf{h},\mathbf{r})) \tag{5}$$

The observed counts were used as the Poisson mean in the poissrnd because they are the maximum likelihood estimators [22]. This method of perturbing observed data for the purpose of quantifying uncertainty is known generally as the parametric bootstrap [23]. These perturbed pole figures were then used to calculate a perturbed ODF $\hat{f}_N(\mathbf{g})$.

An ensemble of perturbed pole figures and perturbed ODFs of size $N$ were calculated. The intensity values of each perturbed ODF were evaluated on a 2.5° regular grid in Euler space. From the ensemble, the mean, absolute standard deviation and relative standard deviation of the intensities were calculated at each grid point and plotted.

The experimental pole figures are shown in Figure 1a. The pole figures are typical of rolled ferritic steel, showing orthotropic sample symmetry from the rolling

process. The relative uncertainty in the pole figure measurements are shown in Figure 1b, calculated using Eq. (3). The relative uncertainty ranges from 1.6% to 13.5%. As expected, regions of higher intensities in Figure 1a correspond to lower relative uncertainty values in Figure 1b, and vice versa. The mean values of the relative uncertainty in the pole figure measurements were 3.76%, 6.64% and 3.26% for the (110), (200) and (211) reflections, respectively.

Figure 2 shows the estimated ODF constructed from the set of experimental pole figures in Figure 1a. The difference between the observed pole figures and those derived from the estimated ODF, reported by the MTEX pole figure to ODF calculation, is 0.83%. The ODF shown in Figure 2 is typical of rolled mild steel. Most of the grain orientations are aligned with the $\gamma$ fiber (normal direction parallel to the $\langle 111 \rangle$ crystal axis; $\phi_1 = 0°$ to 90°, $\Phi = 55.4°$, $\phi_2 = 45°$), indicated by high MUD values along those orientations.

An ensemble size of $N = 5000$ was used in the Monte Carlo analysis. The mean ODF calculated from the ensemble (not shown) was similar to that estimated from experimental pole figures, as shown in Figure 2. Figure 3 shows a difference plot between the mean of the ODF ensemble and the ODF from experimental pole figures.

Figure 4 shows the relative uncertainty in the estimated ODF. The mean relative uncertainty is 1.61% (range 4.01% to 0.52%). The R-Goss orientation $\{011\}\langle 1\bar{1}0\rangle$ (90°, 45°, 0°) shows the highest relative uncertainty, while orientations along the gamma fiber have the lowest values.

Three orientations were investigated in more detail: the R-Goss orientation $\{011\}\langle 1\bar{1}0\rangle$ (90°, 45°, 0°), the $\gamma_1$ orientation $\{111\}\langle 1\bar{1}0\rangle$ (0°, 55°, 45°) and the brass orientation $\{011\}\langle 2\bar{1}0\rangle$ (35°, 45°, 0°). The mean and relative uncertainty values are shown in Table 1. The $N = 5000$ ensemble was broken into two subsets of $N = 2500$ to evaluate the effect of the number of elements in the ensemble.

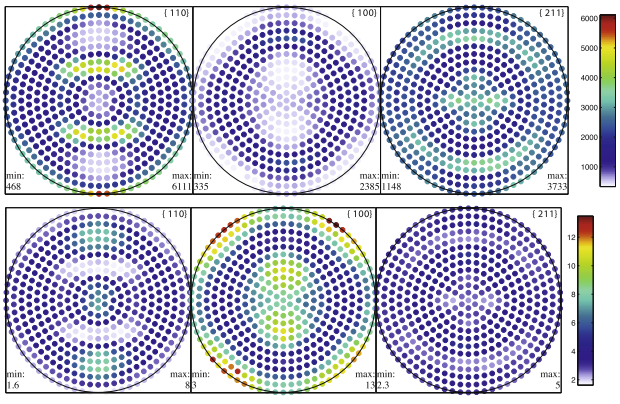


**Figure 1.** (a) (top) Pole figures from (110), (200) and (211) reflections (left to right) generated from neutron diffraction for undeformed SAE 1008 steel. The rolling direction (RD) is the vertical axis and the transverse direction (TD) is horizontal. Pole figures are displayed as number of counts in the peak. (b) (bottom) Relative uncertainty pole figures (%) generated from neutron diffraction data for undeformed SAE 1008 steel.

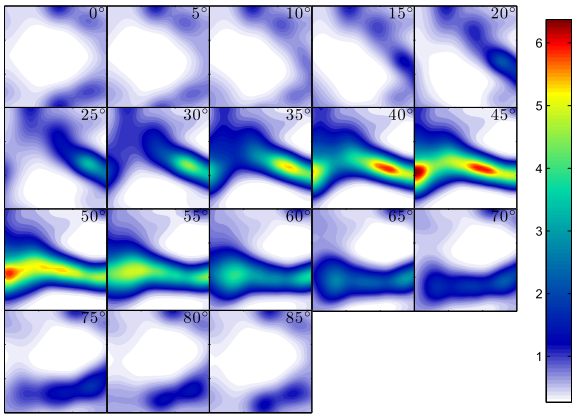


**Figure 2.** ODF constructed from the set of the three input pole figures shown in Figure 1a. Intensity is displayed in units of MUD with Bunge Euler angles. The ODF plot is represented as 18 sections in increments of $\varphi_2 = 5°$ from 0° to 85°, while $\varphi_1$ (along the $x$-axis) and $\Phi$ (along the $y$-axis) range from 0° to 90° in each section.

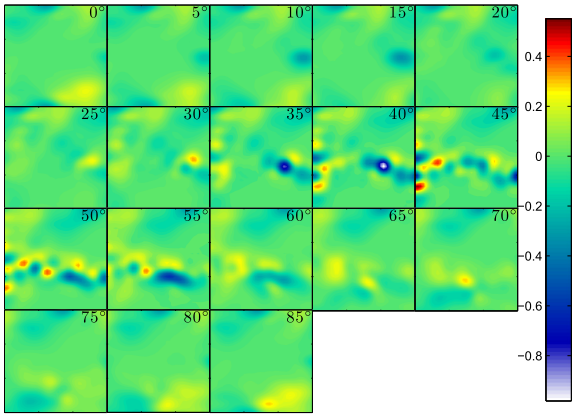


**Figure 3.** Difference between the ODF estimated from experimental pole figures and the mean ODF from ensemble $N = 5000$. The scale is in units of MUD.

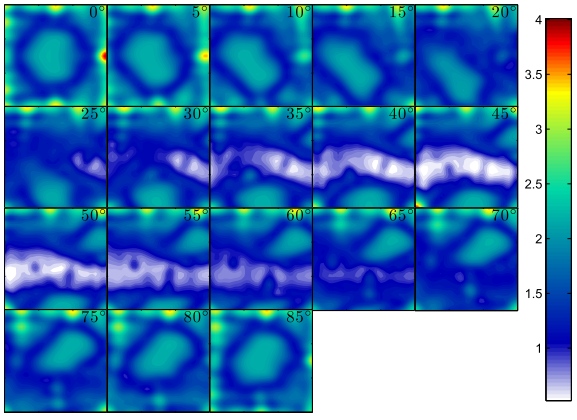


**Figure 4.** Representation of relative uncertainty (%) in the mean ODF using the Euler angle conventions of Figure 2.

The mean relative uncertainty in the estimated ODF, shown in Figure 4, is less than that in any of the pole figures shown in Figure 1b. The uncertainty in the pole figure measurements calculated from this technique is

**Table 1.** Mean and relative uncertainty values at selected orientations.

| | $N = 5000$ | | $N = 2500$ | | $N = 2500$ | |
|---|---|---|---|---|---|---|
| | Mean (MUD) | Relative uncertainty (%) | Mean (MUD) | Relative uncertainty (%) | Mean (MUD) | Relative uncertainty (%) |
| R-Goss | 0.702 | 4.01 | 0.701 | 4.02 | 0.702 | 4.00 |
| $\gamma_1$ | 6.379 | 0.74 | 6.380 | 0.72 | 6.378 | 0.75 |
| Brass | 0.266 | 2.22 | 0.266 | 2.22 | 0.266 | 2.22 |

similar to that observed by Lychagina et al. [10] using the TOF technique. To our knowledge, this is the first estimate of how the uncertainty varies from orientation to orientation in the estimated ODF.

While, in general, there is a trend that larger intensity in the mean ODF results in lower relative uncertainty, this is not always the case. Comparing the R-Goss and brass orientations shows that the brass orientation, despite having a mean intensity of nearly one-third of the R-Goss orientation, has a smaller relative uncertainty.

In summary, a technique to quantify the uncertainty in an estimated ODF by propagating the uncertainty in measured pole figures through the calculation of the estimated ODF was demonstrated. By quantifying uncertainty in an estimated ODF, results can be compared to determine if the difference between two estimated ODFs is statistically significant and comparisons between ODFs can be more rigorous.

The authors acknowledge following people and institutions for their assistance: Dr. Ralf Hielscher at the Chemnitz University of Technology for developing, maintaining and assistance using MTEX; Dr. Antonio Possolo of the Statistical Engineering Division at NIST for introducing the authors to the Monte Carlo technique; the NIST Center for Neutron Research (NCNR) for providing the neutron research facilities used in this work; Dr. William Luecke and Dr. Adam Pintar for their helpful comments; and personnel in the NIST Center for Automotive Lightweighting for helpful discussions. K.S. was supported in part by the Summer Undergraduate Research Fellowship (SURF) program at NIST, together with the National Science Foundation and the NIST-ARRA Undergraduate Fellowship Program.

[1] S. Matthies, H.-R. Wenk, G.W. Vinel, J. Appl. Crystallogr. 21 (1988) 285–304.
[2] U.F. Kocks et al., Texture and Anisotropy: Preferred Orientations in Polycrystals and their Effect on Materials Properties, Cambridge University Press, Cambridge, 2000.
[3] O. Engler, V. Randle, Introduction to Texture Analysis: Macrotexture, Microtexture, and Orientation Mapping, CRC Press, Boca Raton, FL, 2010.
[4] H.J. Bunge, Texture Analysis in Materials Science: Mathematical Methods, Butterworths, London, 1982.
[5] H.J. Bunge, F. Haessner, J. Appl. Phys. 39 (1968) 5503–5514.
[6] S. Matthies, G. Vinel, Phys. Status Solidi B 112 (1982) K115–K120.
[7] K. Pawlik, Phys. Status Solidi B 134 (1986) 477–483.
[8] R. Hielscher, H. Schaeben, J. Appl. Crystallogr. 41 (2008) 1024–1037.
[9] D.I. Nikolayev et al., Mater. Sci. Forum 495–497 (2005) 307–312.
[10] T.A. Lychagina, D.I. Nikolayev, F. Wagner, Texture, Stress, and Microstructure, vol. 2009, Hindawi Publishing Corporation, 2099, pp. 1–10. http://dx.doi.org/10.1155/2009/237485.
[11] A. Mücklich, P. Klimanek, Mater. Sci. Forum 157–162 (1994) 275–286.
[12] S. Matthies, J. Pospiech, Phys. Status Solidi B 97 (1980) 547–556.
[13] S. Matthies, Phys. Status Solidi B 101 (1980) K111–K115.
[14] S. Matthies, G.W. Vinel, K. Helming, Standard Distributions in Texture Analysis, Akademie-Verlag, Berlin, 1987.
[15] A. Morawiec, J. Phys. Condens. Matter 4 (1992) 339–349.
[16] K.G.v.d. Boogaart, Mater. Sci. Forum 495-497 (2005) 179–184.
[17] G.S Fishman, Monte Carlo: Concepts, Algorithms and Applications, Springer, 1996.
[18] Wikipedia. Monte Carlo. <https://en.wikipedia.org/wiki/Monte_Carlo_method>.
[19] P.C. Brand, H.J. Prask, T. Gnaeupel-Herold, Physica B 241–243 (1997) 1244–1245.
[20] S. Matthies, H.R. Wenk, Phys. Status Solidi A 133 (1992) 253–257.
[21] T. Gnaeupel-Herold, BT8 Data Analysis. <http://www.ncnr.nist.gov/instruments/bt8/BT8DataAnalysis.htm>.
[22] G.B. Casella, R.L. Berger, Statistical Inference, Duxbury, Pacific Grove, CA, 2002.
[23] B. Efron, R.J. Tibshirani, An Introduction to the Bootstrap, Chapman & Hall, London, 1993.